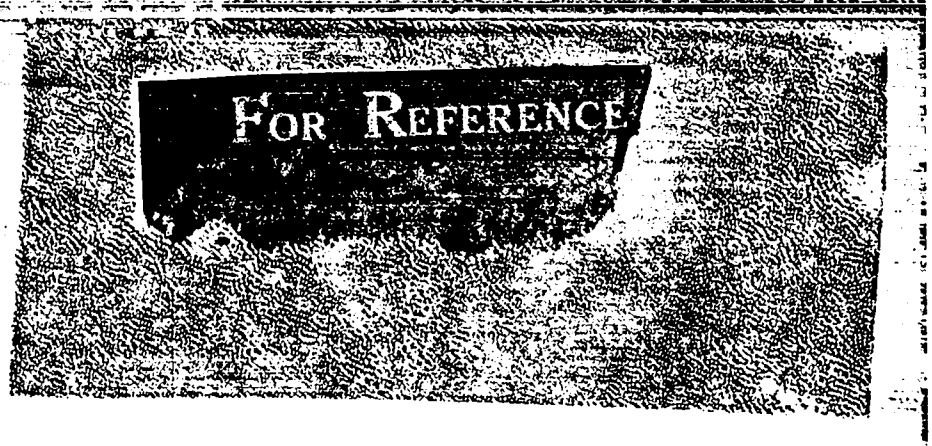

UNCLASSIFIED

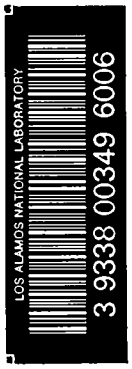

L A Report 18

August 9, 1943

This document contains 30 pages

THE COLLAPSE OF HOLLOW STEEL CYLINDERS BY HIGH EXPLOSIVES

WD - Principles + Testing

WORK DONE BY:

H. Bradner

S. Neddermeyer

J. F. Streib

REPORT WRITTEN BY:

S. Neddermeyer

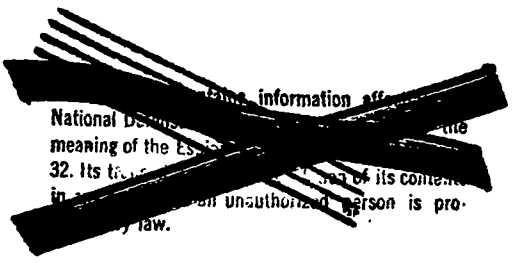

ABSTRACT

Part I gives a very simple approximate one-dimensional treatment of the terminal velocity imparted to a rigid mass by a mass of high explosive. The one-dimensional treatment is presumed to be approximately valid for the cylindrical case provided the charge thickness is small compared to the radius. The result may be expressed to a good approximation by means of the simplified formula $v = \frac{m_e}{m}\sqrt{\frac{2\,u_o}{1+m_e/m}}$, where m_e/m is the ratio (mass of explosive/mass of projectile) and u_o is the initial internal energy per unit mass of the exploded gas, assumed to be initially at uniform pressure and temperature. In Part II the mechanics of the cylinder itself is treated from simple energy arguments using the assumption of a constant yielding stress, and the result of Part I is applied to estimate the attainable collapse ratio as a function of the mass ratio of explosive and cylinder. In Part III a few new experimental data are considered. The observed collapse ratios are found to be in rough agreement with the ones calculated for RDX if one assumes an effective yielding stress of 300,000 lb/in^2. The observed mass ratios for TNT are however found to be high by as much as 50%. The discrepancy can be attributed to several things: (a) The theoretical mass ratios are only approximate and are probably too low. (b) The assumed value for the yielding stress for steel (10-20 carbon, cold drawn) may be too high and may have a lower effective value when the collapse is rapid than when it is slow. The origin of the discrepancy can be settled by measurements of the rate of collapse, or by direct measurements of heat generation. These experiments are now in progress.

THE COLLAPSE OF HOLLOW STEEL CYLINDERS BY HIGH EXPLOSIVES

I. MAXIMUM VELOCITY GIVEN TO A PROJECTILE

A correct treatment of the motion imparted to a projectile by a charge of high explosive involves a number of factors which complicate the dynamical problem of taking into account simultaneously the motions of the whole system of projectile plus exploded gas: (a) The equation of state is rather complicated because of the extreme initial pressure and density. (b) The equilibrium of combustion products presumably shifts as the hot gas expands, and (c) The detonation wave leaves the exploded gas with a residual momentum and a non-uniform pressure distribution. A very rough preliminary treatment which is of some use in correlating experimental data may be given on the following basis. (a) The motion is assumed to be one-dimensional. This should be a fair approximation for "implosions" of cylindrical or spherical shells in which the charge thickness is small compared to the radius. (b) The detonated explosive is assumed to be initially an ideal gas at uniform pressure and density. (c) The projectile is assumed to remain at rest while receiving the impulse from the explosive. Assumption (b) is presumably a fair approximation if the explosive is detonated in several directions at once, and (c) can be valid only for small ratios, m_o/m, of explosive mass to projectile mass.

On this basis we assume that only the boundary layers of the detonated explosive move, forming a discontinuous shock wave in the outside air and a discontinuous rarefaction wave moving into the exploded gas which is assumed to maintain the initial pressure p_o until the rarefaction wave

passes. The last assumption is not a valid one as the rarefaction wave cannot remain discontinuous, but is used only as a crude approximation to represent some kind of an average motion of the wave front. A rigorous solution for the case of an ideal gas is given by Streib in another report.

Referring to Fig. 1b, we then assume that there are three regions of constant pressure p_o, p' and the outside atmospheric pressure p_1, that rarefaction and shock waves travel with constant velocities v, v'_1, and that the boundary between expanded gas and compressed air travels with constant velocity v'. The conservation laws for mass, momentum and energy may be written down in the form:-

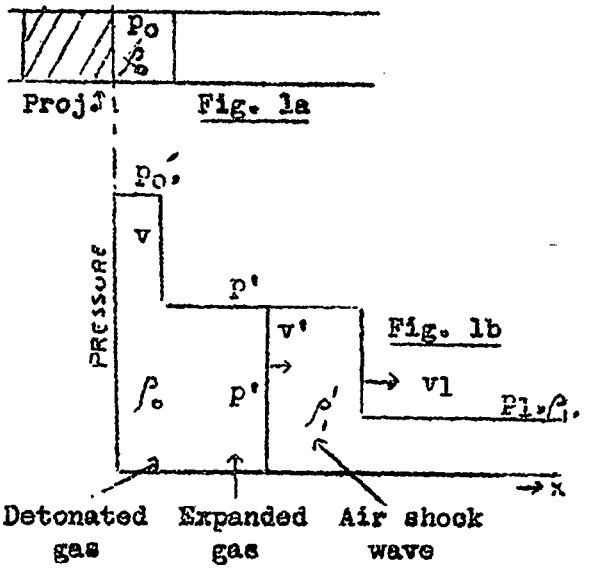

(1) $$\rho_o v = \rho'(v + v')$$

(2) $$p_o - p' = \rho_o v v'$$

(3) $$\frac{1}{\gamma - 1} p_o v = \left(\frac{1}{\gamma - 1}\frac{p'}{\rho'} + \frac{v'^2}{2}\right)\rho_o v + p' v'$$

} Rarefaction front

(4) $$\rho_1 v'_1 = \rho'_1 (v_1 - v')$$

(5) $$p' - p_1 = \rho_1 v' v'_1$$

(6) $$\left[\frac{1}{\gamma - 1}\left(\frac{p'}{\rho'_1} - \frac{p_1}{\rho_1}\right) + \frac{v'^2}{2}\right]\rho_1 v'_1 = p' v' - p_1 v'_1$$

} Shock front

Here $\frac{1}{\gamma - 1}\frac{p}{\rho} = u$ is the internal energy per unit mass.

These are readily solved for the two equations in v':-

$$v'^2 = \frac{x + \gamma - 2}{\frac{\gamma}{\gamma - 1}\frac{x}{x - 1} - \frac{1}{2}} u_1 = \frac{(1 - \mu x)}{\frac{\gamma}{\gamma - 1}\frac{\mu x}{1 - \mu x} + \frac{1}{2}} u_o$$

where $u_1 = \frac{1}{\gamma - 1}\frac{p_1}{\rho_1}$ $\qquad u_o = \frac{1}{\gamma - 1}\frac{p_o}{\rho_o}$

and $x = \frac{p'}{p_1}$; $\mu = \frac{p_1}{p_o}$; $\mu x = \frac{p'}{p_o}$.

Now $x >> 1$ and $\mu x << 1$ so that to a good approximation

$$v' = \sqrt{2u_o} \qquad \text{and} \qquad x = \frac{\gamma + 1}{\gamma - 1} \cdot \frac{u_o}{u_1}$$

and the velocity of the rarefaction wave is

$$v = \frac{p_o - p'}{\rho_o v'} \simeq \frac{p_o}{\rho_o v'} = (\gamma - 1)\sqrt{\frac{u_o}{2}}$$

Thus from the equation for v'^2 we see that the kinetic energy of the expanding gas comes out to be approximately equal to the initial internal energy of the detonated explosive. Tables 1 and 2 give some applicable data for several different explosives. As the ideal-gas relation for the internal energy $u_o = \frac{1}{\gamma - 1}\frac{p_o}{\rho_o}$ is not applicable to the highly compressed explosive gas we make direct use of the calorimetric measurements of the energy of explosion and put this equal to u_o.

TABLE 1. MEASURED HEATS OF EXPLOSION (for loading density 1.5)
(Kistiakowsky, OSRD # 293)

EXPLOSIVE	HEAT OF EXPLOSION	DETONATION VELOCITY (meas.)
TNT	650 cal./g/	6700 meters/sec
Tetryl	890	7200
PETN	1410	7600
Cyclonite (RDX)	1240	7800

TABLE 2. PROPERTIES OF PRODUCTS OF ADIABATIC CONSTANT-VOLUME EXPANSION
(Calculated) (Brinkley and Wilson, OSRD # 1231)

EXPLOSIVE	LOADING DENSITY	TEMPERATURE	PRESSURE
RDX, Comp B	1.61	3140° K	98.8×10^9 dynes/cm^2
TNT	1.46	2910°	65.4
50/50 Amatol	1.58	2480°	79.8

For RDX, density 1.5, one then gets

$$x = \frac{p'}{p_1} = 163$$

$$\frac{1}{\mu x} = \frac{p_o}{p'} = 610$$

$$v' = 3.2 \times 10^5 \text{ cm/sec.}$$

$$v = 0.65 \times 10^5 \text{ cm/sec.}$$

The total momentum given to the projectile per unit sectional area will then be, for small charges of length l_o

$$P = p_o l_o / v = \rho_o l_o v' = m_o v'.$$

Alternatively,

(7) $$v_p = \frac{m_o}{m} v' = \frac{m_o}{m}\sqrt{2u_o}$$

is the maximum velocity imparted to the projectile of mass m per unit sectional area.

This suggests that a somewhat better result may be obtained by a direct overall application of the conservation laws, if one assumes the internal energy to be divided between projectile and ejected gases. The equations are

$$m_o u_o = \frac{m_o}{2} v'^2 + \frac{m}{2} v^2$$

$$m_o v' = mv.$$

The solution is

$$(8) \qquad v = \frac{m_o}{m} v' = \frac{m_o/m}{\sqrt{1 + m_o/m}} \sqrt{2u_o}$$

This is plotted in Fig. 2 for RDX and TNT using the measured values of u_o from Table 1. In the figures and in all that follows the notation m_e, ρ_e, r_e, ℓ_e has been used for the mass, density and dimensions of the explosive charge.

II. MOTION OF THE CYLINDER

The pressure existing in a detonated high explosive is of the order of 10^6 lb/in^2, which is much higher than the yielding strengths of any ordinary metals. In treating the motion of a collapsing shell we therefore assume that there is plastic flow against a constant yielding stress throughout the shell.

For the simple preliminary treatment we ignore volume changes and therefore any effects of elastic waves. The shell is assumed to receive an initial inward impulse from the pressure p_o and thereafter to move freely against the yielding stress. This assumption is not quite valid because the velocity of the rarefaction wave into the exploded gas is $\sim .6 \times 10^5$ cm/sec., which is of the same order as the velocity attained by the shell; this should not however seriously invalidate the results. The motion may then be treated by the energy equation $K = K_o - W$ where K is the

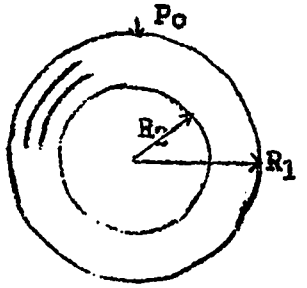

kinetic energy of the shell at any stage of the motion, K_o is the initial kinetic energy, and W is the work done at that stage against the internal stress. If W and K_o are known then the velocities of the inner and outer surfaces can be calculated as a function of the collapse ratios. K_o is calculated from Equation (8). In applying Equations (7) and (8) as approximations to a cylindrical or spherical case it may be noted that in (7) the mass ratio should be taken as $\rho_e t_e/\rho t$ where t_e and t are the thicknesses of explosive and shell, whereas in (8) one should presumably take the actual mass ratio. However, since (8) approaches (7) for small mass ratios and must in any case represent an upper limit, we have used $m_e/m = \rho_e t_e/\rho t$ in all that follows. In the worst case this is about 0.6 the actual mass ratio.

Work of collapse

The pressure required to deform a thin cylindrical shell of radius r and thickness Δr, against a constant yielding stress s, is

$$p = \frac{s\Delta r}{r}.$$

If the volume change is neglected then the volume of the thin shell is $\Delta V = 2\pi r \Delta r = \text{const.}$, and the work required to collapse the shell to a radius r' is

$$\Delta W = -\int_{r}^{r'} 2\pi r p dr = s\Delta V \int_{r}^{r'} dr/r = s\Delta V \ell n(r/r').$$

Let R_1, r_1 be the initial and final outside radius and R_2, r_2 the initial and final inside radius. The total work to collapse a thick shell from R_1, R_2 to r_1, r_2 is

$$W = s \int \ell n \frac{r}{r'} dV.$$

If we use the constant-volume relation

$$r^2 - R_2^2 = r'^2 - r_2^2; \quad R_1^2 - R_2^2 = r_1^2 - r_2^2$$

$$W = \frac{\pi s}{2} \int_{r_2}^{r_1} \ell n \frac{R_2^2 - r_2^2 + r'^2}{r'^2} \, d(r'^2)$$

with the notation

$$\lambda = \frac{R_2}{R_1}; \quad x = \frac{r_1}{R_1}; \quad y = \frac{r_2}{R_1}, \quad \text{(called the "inner collapse ratio")}$$

the total work per unit mass w, may be written

$$(9) \qquad w = \frac{W}{M} = \frac{s/2\rho}{1 - \lambda^2} \left\{ y^2 \ell n y^2 - x^2 \ell n x^2 - \lambda^2 \ell n \lambda^2 \right\}.$$

Here x, y and λ are related by the constant-volume condition

$$x^2 - y^2 = 1 - \lambda^2.$$

In Fig. 3, $w/(s/2\rho)$ is plotted as a function of y for two values of λ. We put $w = v^2/2$ where v is the equivalent initial velocity to produce the collapse ratio y and in Figs. 4 and 5 we plot v against y for three values of the yielding stress and for two values of λ. For these curves $\rho = 7.5$, whereas it should be about 7.8 for the steel cylinders of Part III. The curves of Figs. 6, 7 were derived from Figs. 4, 5 by using Fig. 2 to convert equivalent initial velocity to mass ratio.

Rate of collapse

The kinetic energy may be shown to be

$$K = \frac{Mv_2^2}{2} \frac{y^2}{1 - \lambda^2} \ell n \frac{x^2}{y^2} + \frac{Mv_2^2}{2} f(y)$$

where v_2 is the velocity of the inside surface, and x, y and λ are connected by the same constant volume condition as before: $x^2 - y^2 = 1 - \lambda^2$. If we write $w = (s/2\rho)g(y)$ then the energy equation is

$$(v_2^2/2)\, f(y) = v_o^2/2 + (s/2\rho)\, g(y).$$

This may be used to find v_2 as a function of y for any assumed value of v_o^2. For the case of "critical collapse" $f(0) = 0$, so $v_o^2 = -(s/\rho)\, g(0)$. The kinetic energy function f(y) is plotted in Fig. 8 for various values of λ, and in Fig. 9 the inner velocity for the critical case has been plotted as a function of collapse ratio with $\lambda = .667$, $s = 300{,}000$ lb/in^2. The inner velocity is also shown for the same initial velocity, but no resisting stresses. In this case $v_2 = v_o/\sqrt{f(y)}$.

III. EXPERIMENTAL RESULTS

For the preliminary experiments, which were of necessity done with meagre equipment, the aim has been first to observe the main features of the phenomena when metal shells undergo extreme and rapid plastic flow under external pressure, and to make an empirical determination of the relation between collapse ratio and mass ratio. These experiments are being followed by observations of the velocities and times of collapse, for which several direct methods have been devised.

About 30 experiments have been carried out with mild steel cylinders ranging in diameter from 3" to 6 5/8" and in wall thickness from $\frac{1}{4}$" to $1\frac{1}{2}$". The explosive used first was TNT crystals packed to a density of about 0.87 g/cm^3, and in all the later experiments, a plastic explosive called "Composition C", which is a mixture of finely powdered RDX (88%), also called "Cyclonite", and vegetable oil (12%). An assembly typical of that usually used is shown in Fig. 10, which is drawn to scale for Experiment # 26.

The results of 16 experiments are listed in Table 3 in which the figure numbers correspond to the photographs. The experiment numbers are marked on the samples in the photographs. All the analyzable data are included in Table 3, as well as a number of typical examples of the sort of fragmentation occurring when large charges are used.

Analysis of the data; stability of collapse

The greatest difficulty in obtaining interpretable experimental results arises from the instability which necessarily exists when the wall thickness is small compared to the radius. This is further enhanced by the non-uniform pressure left by the detonation wave. The detonation wave effect can be reduced by using multiple detonations, started simultaneously by tying several primacords of the same length to one blasting cap; four detonation points, spaced evenly around the circumference at the middle of the cylinder, were used in most cases (see Fig. 10). The effect of the non-uniform pressure left by the detonation wave is shown very strongly in Fig. 14 (Exps. 9 and 11) where there were four evenly spaced detonation points at the ends of the cylinders (at the bottom in the photograph). Even when several detonation points are used there is usually evidence of greater action in the region between detonation points. There are almost always sharply defined lines, along which the detonation waves come together, showing at least a slight etching of the metal and in several cases a strong tendency to shear. This is shown expecially well in Figs. 12 and 13. When shearing rupture occurs it is usually along a surface making an angle of about 45° with a radial plane, which is the direction in which the strain is a simple shear (also in which the shearing strain and stress are a maximum).

It seems likely that fairly uniform collapse can be produced by using a sufficiently large explosive charge; this conclusion follows from the fact that the pressure exerted by the explosive is large compared to the

strength of the material, and if the shells are given a large enough inward momentum the stresses should play a relatively small part. Experimental evidence for this is shown in Figs. 11, 15, 16, 18 and 19. In Fig. 11, Exp. 1, for example, the steel tube was 3" diameter, $\frac{1}{4}$" wall, with a 3/4" charge of TNT crystals; Exp. 7 was the same except that the charge was $1\frac{1}{2}$" thick. In the first case the tube collapsed more or less uniformly until the wall had thickened to about 5/16", then ruptured into a number of strips which went into an irregular bundle. In the second case the collapse was evidently quite uniform but so violent that the tube bounced out again and fragmented. The thin-walled copper tube of Fig. 15, Exp. 5 is another striking example of the same thing.

In attempting to interpret the data by means of the curves of Figs. 6, 7, only the cases of partial collapse, or else complete collapse without fragmentation could be used. In cases where the collapse was non-uniform, or where rupture occurred, an attempt was still made to estimate the collapse ratio by getting a rough average of the wall thickness. This was done even in the case of Fig. 1, Exp. 1, on the grounds that the work done in the initial thickening of the wall was probably large compared to the work of collapsing the bundle of ruptured strips. The mass ratios $\rho_e h_e / \rho h$ actually used and the ones calculated are listed in Table 3. Five points having $\lambda = .667$ or $.833$ are marked with (*) and plotted in Fig. 6 or 7.

The yielding stress; time of collapse

There is no sound basis for choosing to interpret the data in terms of a yielding stress of 300,000 lb/in^2. This value was quoted to the writer in private conversation as an approximate experimental result for extreme and very rapid deformation, which appeared to be more or less independent of the heat treatment the steel had received. As this value appeared to fit the data for Composition C it was chosen as a reasonable value, although likely to be high. Independent checks of the effective values of s are to

be made both by calorimetric measurement of the heat of working and by measurements of the rate of collapse.

Two preliminary measurements of the time of collapse, made by a bullet-catching method devised by Streib, for a 3" OD, $\frac{1}{2}$" wall steel cylinder with a $\frac{1}{2}$" charge of Composition C gave times of about 10^{-4} sec. The expected value would be about half this on the basis of 300,000 lb/in^2. These first experimental values should be however essentially upper limits, and further measurements by this and other methods will be the subject of a later report by Streib.

Velocities of projectiles fired with small charges of high explosive

To get some independent information on the relation between terminal velocities and mass ratios, some experiments have been begun by Bradner and Bloch, in which 2" diameter steel projectiles were fired upward with varying charges (confined only by pasteboard and thin wood) of pentolite of the same diameter, pressed to a density 0.45 g/cm^3. Velocities were determined by measuring the time of flight with a stop watch. The data for two projectile sizes are plotted in Fig. 20.

A very rough interpretation of these experiments can be given in terms of the simple one-dimensional theory of Sec. I, if we assume that immediately after detonation the rarefaction wave travels inward from the two free surfaces of the detonated explosive with the same constant velocity. We then assume that the initial pressure p_o acts on the surface of the projectile at any point only until the rarefaction reaches that point, and that the pressure is thereafter negligible. With these simple assumptions we can compute the ratio of the momentum imparted to the projectile to the momentum it should have got if the explosive were free to expand only from the free end surface.

We get for this ratio

$$P/P_1 = r_e/3l_e \qquad \text{for } r_e < l_e$$
$$= 1 - l_e/r_e + l_e^2/3r_e^2 \qquad \text{for } r_e > l_e,$$

where r_e = radius of projectile and charge, and l_e = length of charge. This factor is applied to the result of the one-dimensional calculation to get the curves of Fig. 20 appropriate to the projectile masses used. Good agreement cannot be expected, but the curves do seem to represent the trend of the experimental data. More complete results will be given in a later report by Bloch and Bradner.

TABLE 3. SUMMARY OF PRINCIPAL RESULTS

Notation: R_1, R_2 = Initial outer, inner radii; r_1, r_2 = final outer, inner radii

$\lambda = R_2/R_1$

y = "Inner" collapse ratio r_2/R_1

h_e, ρ_e, h, ρ = thicknesses and densities of explosive and cylinder.

		CYLINDER					EXPLOSIVE				
										$\rho_e h_e/\rho h$	
Fig.	Exp. no.	Material	R_1	R_2	λ	y	Material	h_e	ρ_e	used	calc. from y
			in.	in.				in.			
11	1*)	Steel	1.50	1.25	0.833	0.633	TNT	0.75	0.87	0.28	.17
	7[2]	Steel	1.50	1.25	0.833	0 [2]	TNT	1.50	.87	.67	> .40
12	2*)	Steel	1.50	1.00	.667	.553	TNT	.75	.87	.167	.12
	10*)	Steel	1.50	1.00	.667	.23	TNT	1.50	.87	.32	.26
13	3	Steel	2.00	1.00	.500	.408	TNT	1.00	.87	.11	.11
	4	Steel	2.00	1.50	.750	.601	TNT	1.00	.87	.22	.14
14	9[1]	Steel	1.50	.75	.500	.17[1]	TNT	1.50	.87	.22	--
	11[1]	Steel	1.50	1.00	.667	~.10[1]	TNT	1.50	.87	.33	--
15	6	Bronze	1.640	1.047	.638	~.27	TNT	1.36	.87	.23	--
	5[2]	Copper	1.750	1.531	.875	0 [2]	TNT	1.25	.87	.56	--
16	13[2]	Steel	1.50	1.00	.667	0 [2]	Comp. C	1.50	1.49	.57	> .2
	14[2]	Steel	1.50	.75	.500	0 [2]	Comp. C	1.50	1.49	.38	> .15
17	18[2]	Steel	2.00	1.00	.500	0 [2]	Comp. C	1.00	1.46	.19	.15
18	26*)	Steel	3.00	2.00	.667	~.37	Comp. C	.75	~1.5	.14	.14
19	21*)	Steel	3.00	2.00	.667	0	Comp. C	1.00	1.59	.20	.20
20	22	Steel	3.00	2.00	.667	0	Comp. C	1.00	~1.5	.19	.20

*) Plotted as an experimental point in Fig. 6 or 7.
1) Detonated from lower end. Measured at section of maximum collapse.
2) Collapsed and fragmented.

[redacted]

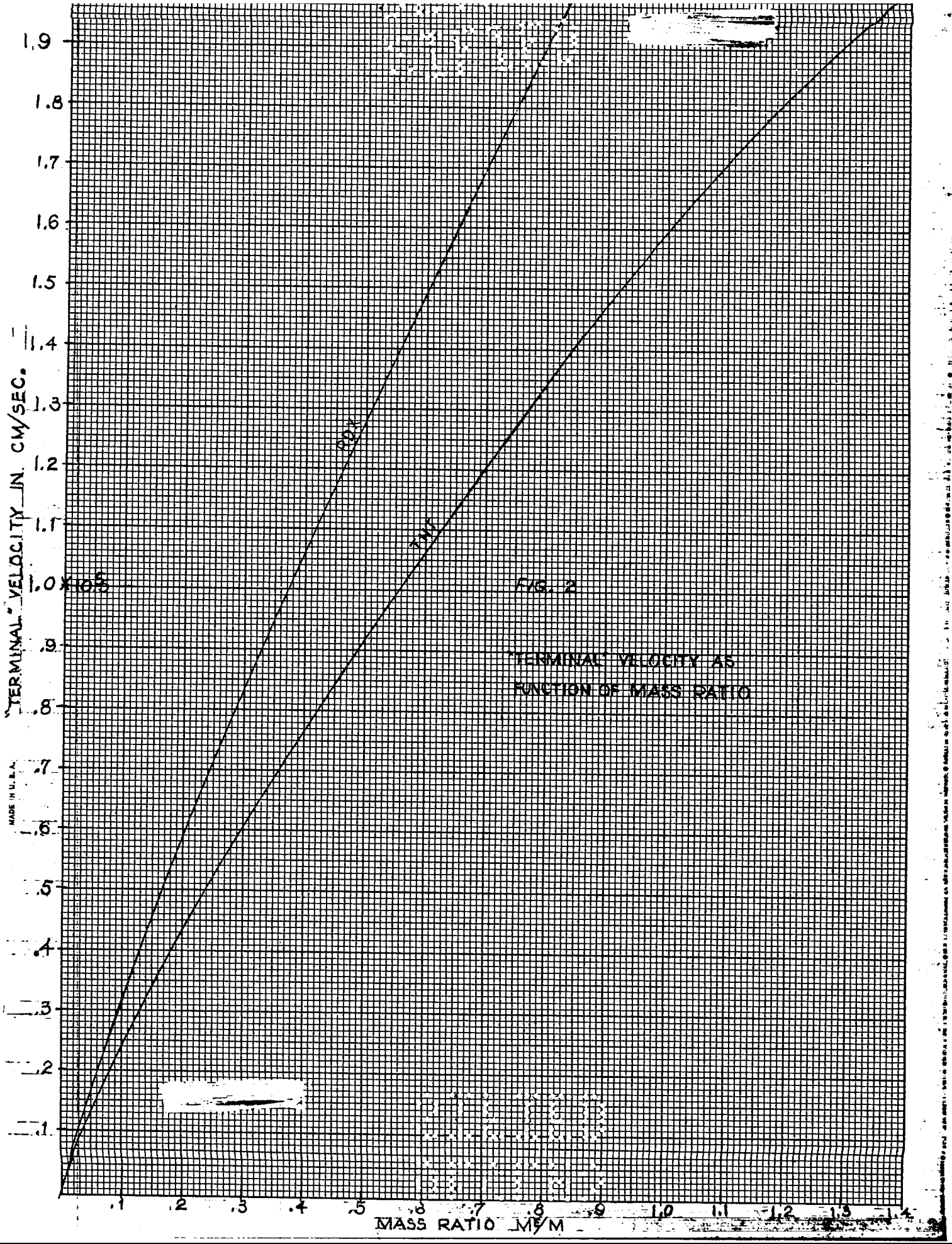

FIG. 2

TERMINAL VELOCITY AS FUNCTION OF MASS RATIO

FIG. 3

WORK OF COLLAPSE AS FUNCTION OF INNER COLLAPSE RATIO (CYLINDRICAL CASE.)

$y = \Delta_2/R_1$

$x = R_2/R_1$

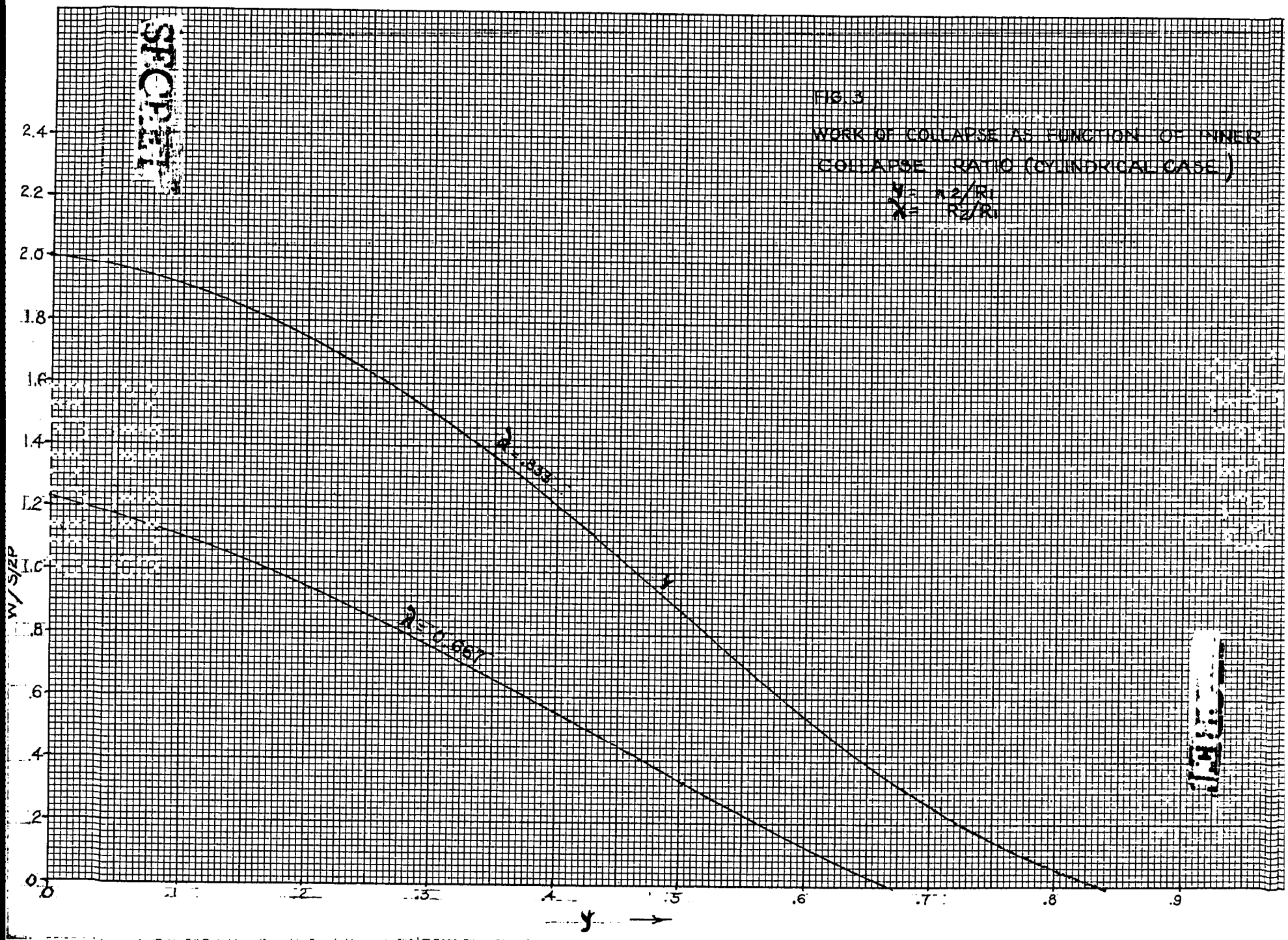

FIG. 4

EQUIVALENT INITIAL VELOCITY
VS. COLLAPSE RATIO
(CYLINDRICAL CASE)
$R_2/R_1 = 0.667$ $\beta = 7.5$

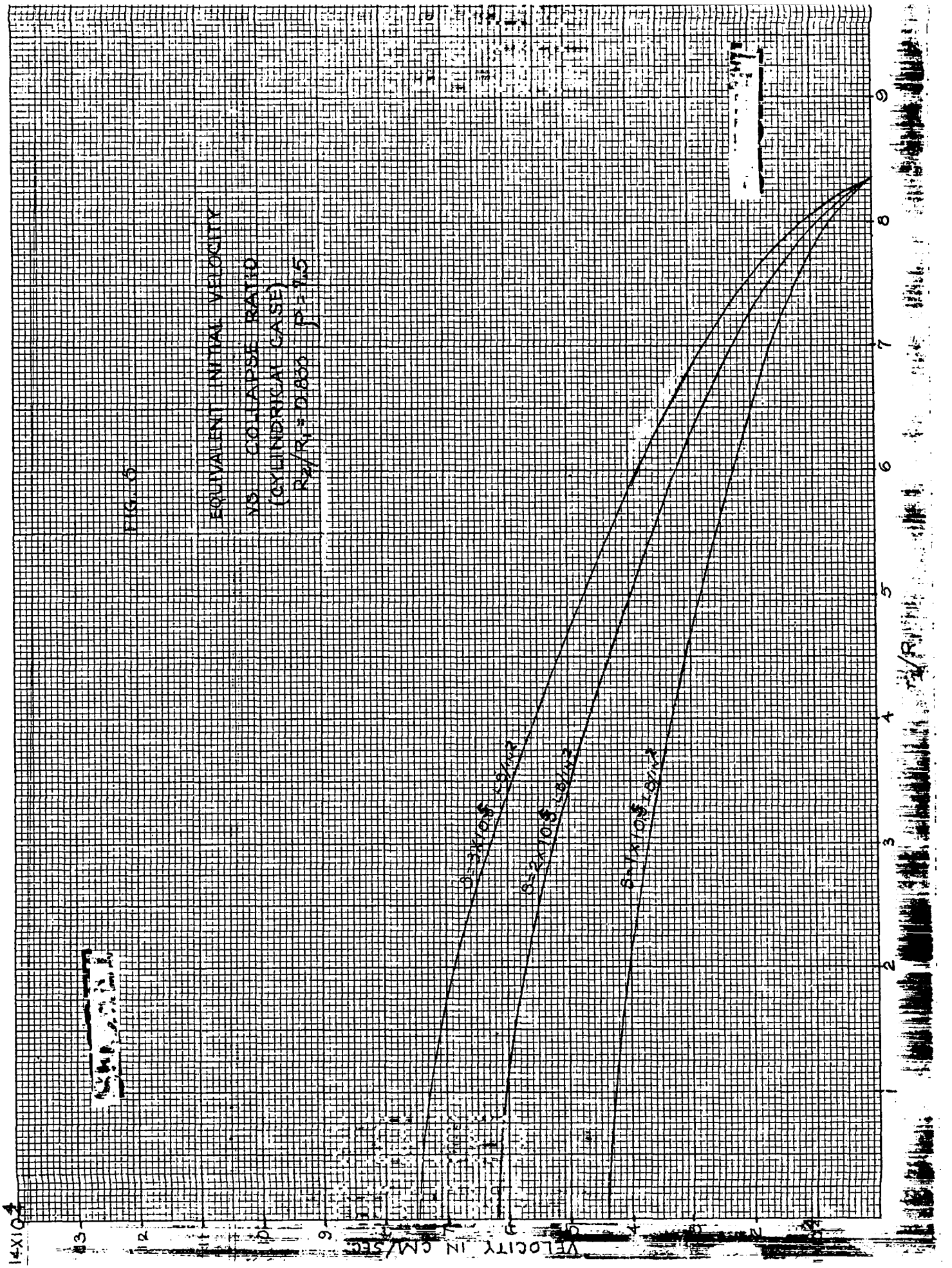

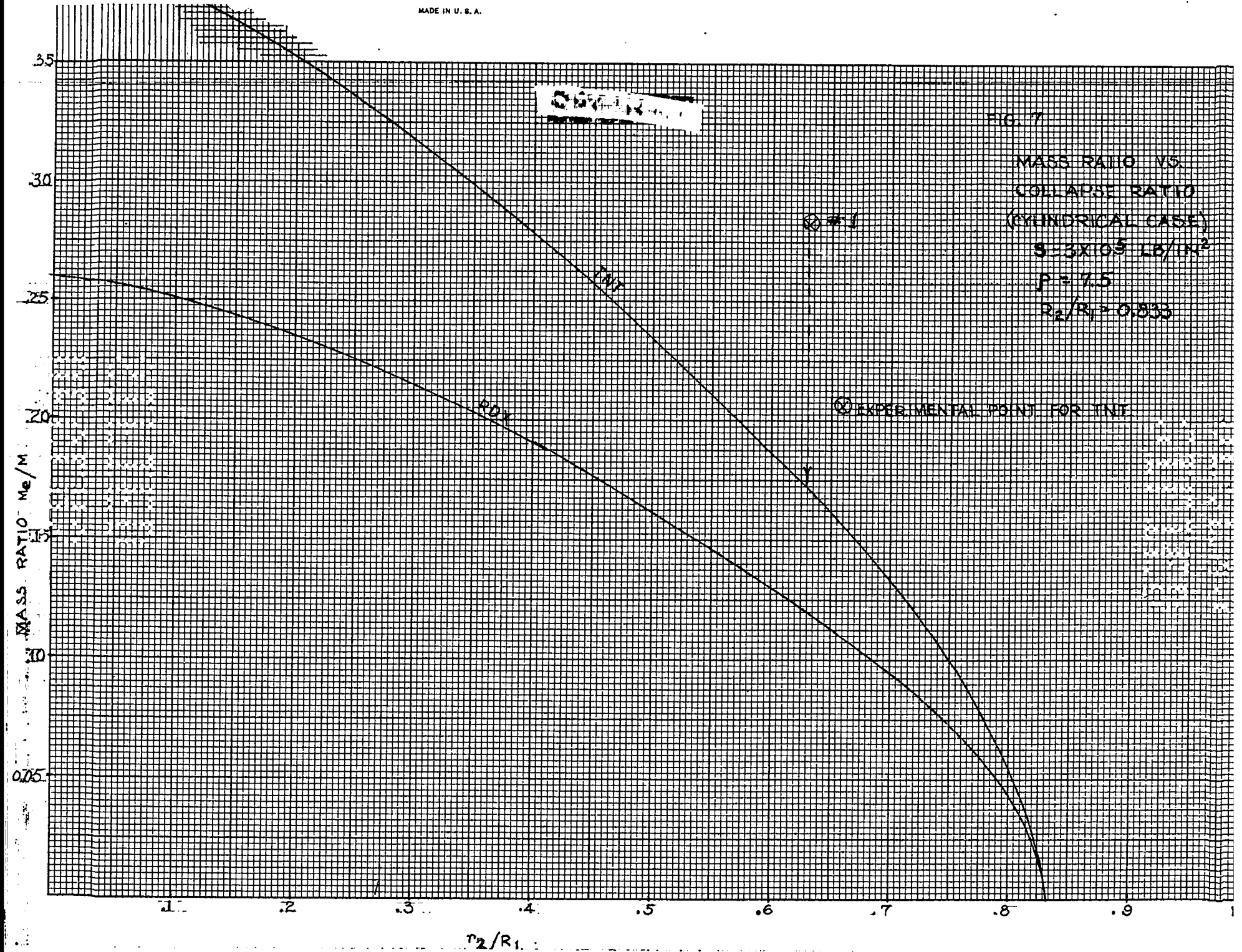

FIG. 7

MASS RATIO VS. COLLAPSE RATIO (CYLINDRICAL CASE)

$S = 3 \times 10^5$ LB/IN^2

$\gamma = 1.5$

$R_2/R_1 = 0.833$

APPROVED FOR PUBLIC RELEASE

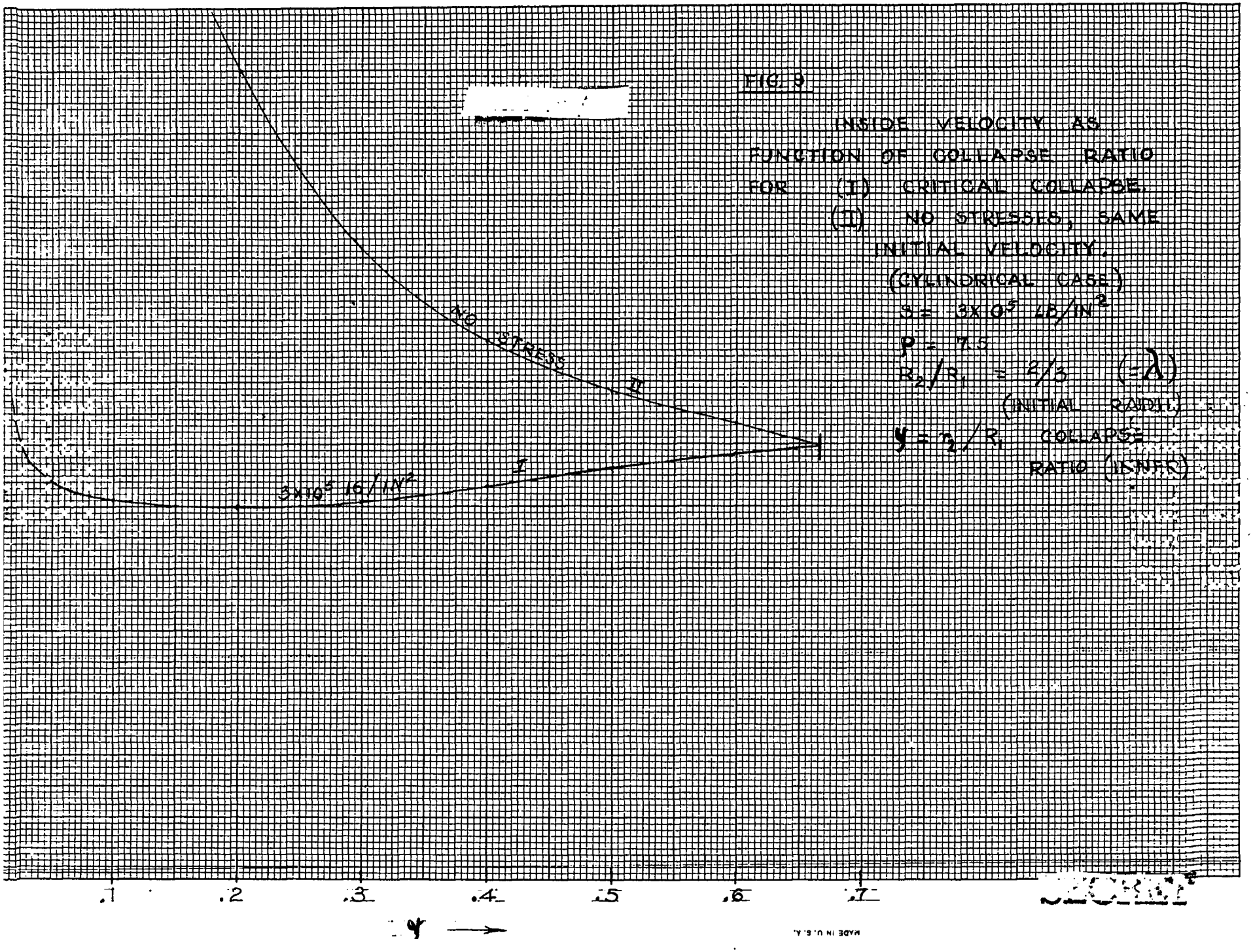

FIG. 9

INSIDE VELOCITY AS FUNCTION OF COLLAPSE RATIO FOR (I) CRITICAL COLLAPSE. (II) NO STRESSES, SAME INITIAL VELOCITY. (CYLINDRICAL CASE)

$S = 3\times10^3$ LB/IN^2

$\rho = 7.5$

$R_2/R_1 = 2/3$ $(=\lambda)$ (INITIAL RADII)

$\gamma = R_2/R_1$ COLLAPSE RATIO (USUAL)

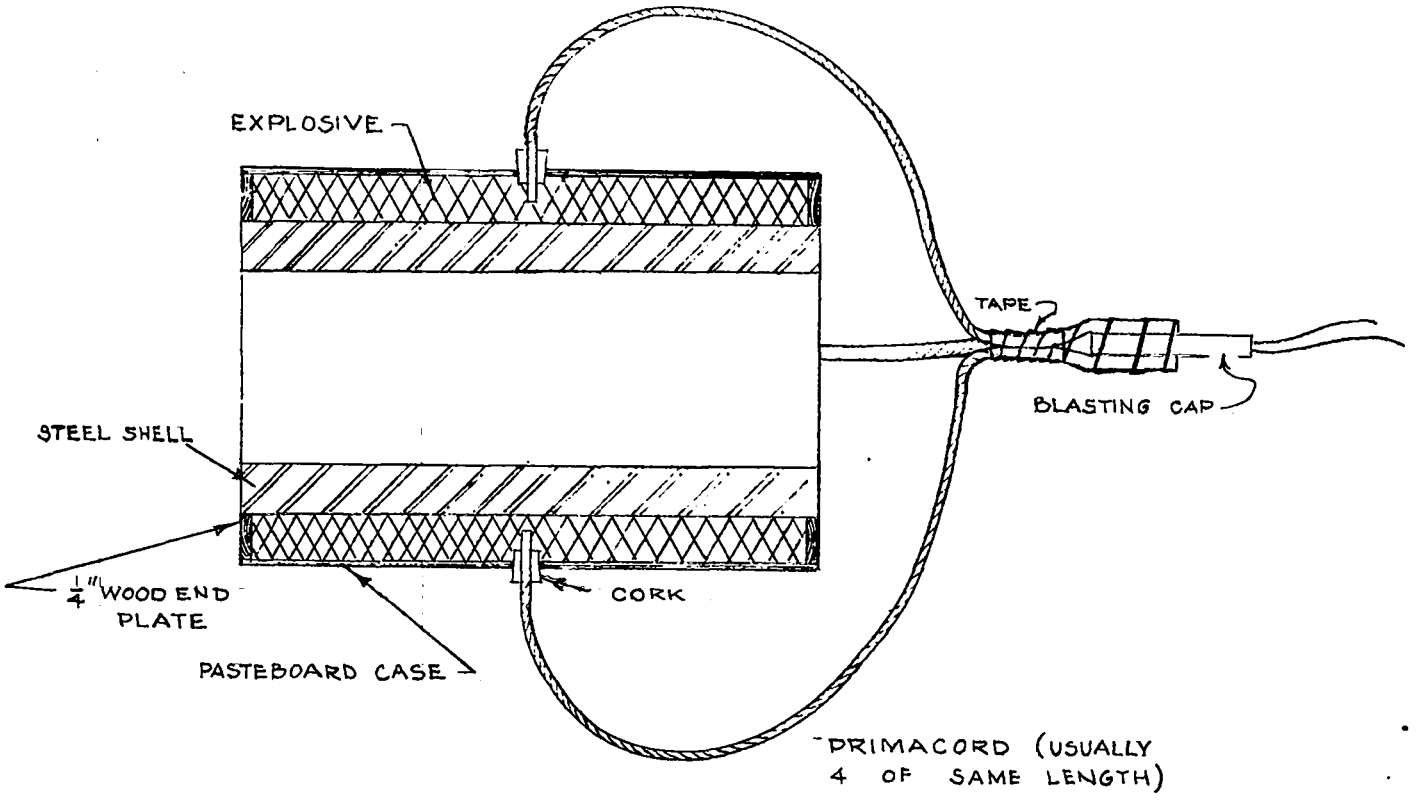

FIG. 10

SECTION OF TYPICAL ASSEMBLY
DRAWN TO SCALE OF EXPERIMENT # 26

The detailed data are given in Table 3. Experiment numbers are marked on the samples in the photographs. In each photograph the original size of the sample is shown by a ring or a complete cylinder. All cylinders are seamless 30-40 carbon steel tubing with a static yield point of about 55000 lb./in^2. Four-point detonation at center unless otherwise stated. Loading density for TNT, 0.87; for Comp. C, about 1.5.

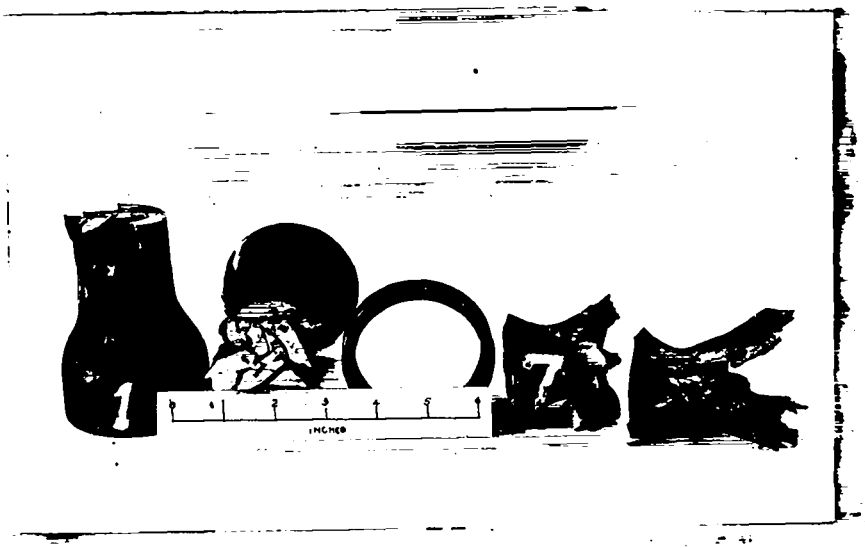

Fig. 11. Exp. 1: 3" OD, ¼" wall, 8" long
TNT ⅜" thick, 6" long.

The boundary of the explosive charge can be seen etched on the cylinder.

Exp. 7: Same except TNT 1½" thick, 7½" long.

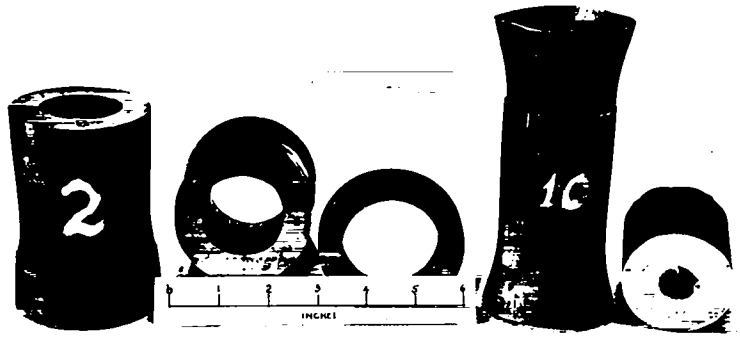

Fig. 12. No. 2: 3" OD, $\frac{1}{2}$" wall, 8" long
TNT $\frac{3}{4}$" thick, 6" long

No. 10: Same except TNT $1\frac{1}{2}$" thick, $7\frac{1}{2}$" long
No. 2 increased in length about $\frac{1}{4}$" and No. 10 about $\frac{3}{4}$"

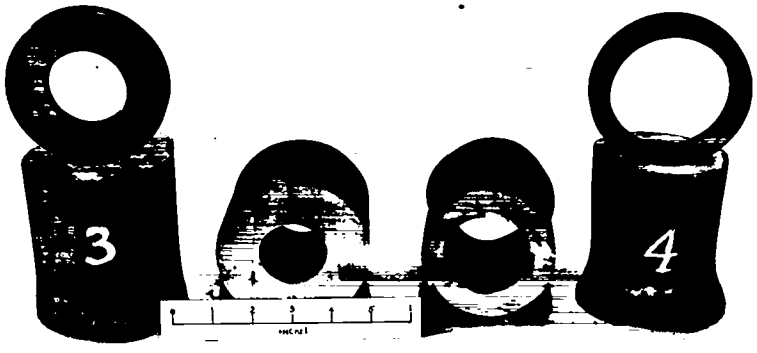

Fig. 13. Exp. 3: 4" OD, 1" wall, 8" long
TNT, 1" thick, $7\frac{1}{2}$" long

Exp. 4: 4" OD, 1" wall, 8" long
TNT, 1" thick, $7\frac{1}{2}$" long

Shearing rupture is shown along lines where detonation waves meet.

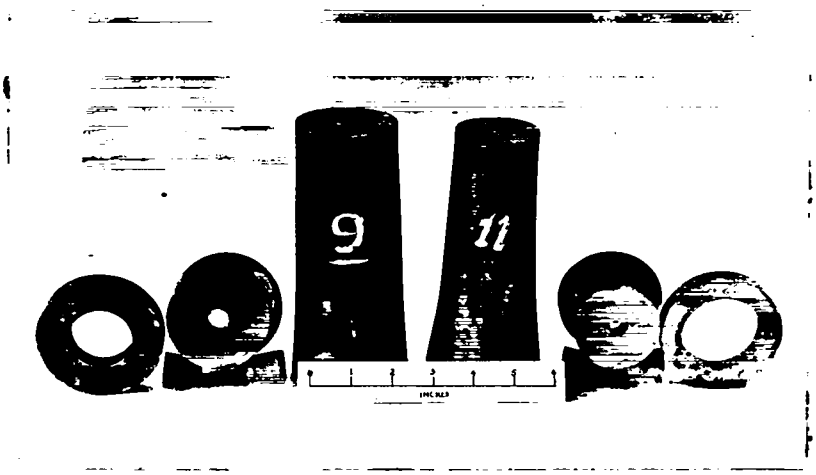

Fig. 14. Exp. 9: 3" OD, $\frac{3}{4}$" wall, 8" long
TNT, $1\frac{1}{2}$" thick, $7\frac{1}{2}$" long

Exp. 11: 3" OD, $\frac{1}{2}$" wall, 8" long, same charge

Both detonated from 4 points at lower end in photograph

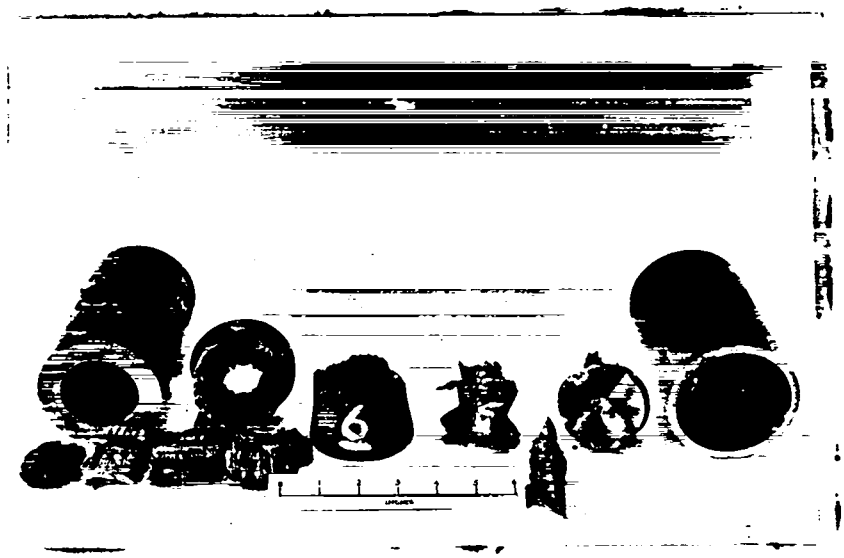

Fig. 15. Exp. 6: Bronze, 3.281" OD, 0.593" wall, 6" long
TNT, 1.36" thick, $5\frac{1}{2}$" long

Exp. 5: Copper, $3\frac{1}{2}$" OD, 7/32" wall, 6" long
TNT, $1\frac{1}{4}$" thick, $5\frac{3}{4}$" long

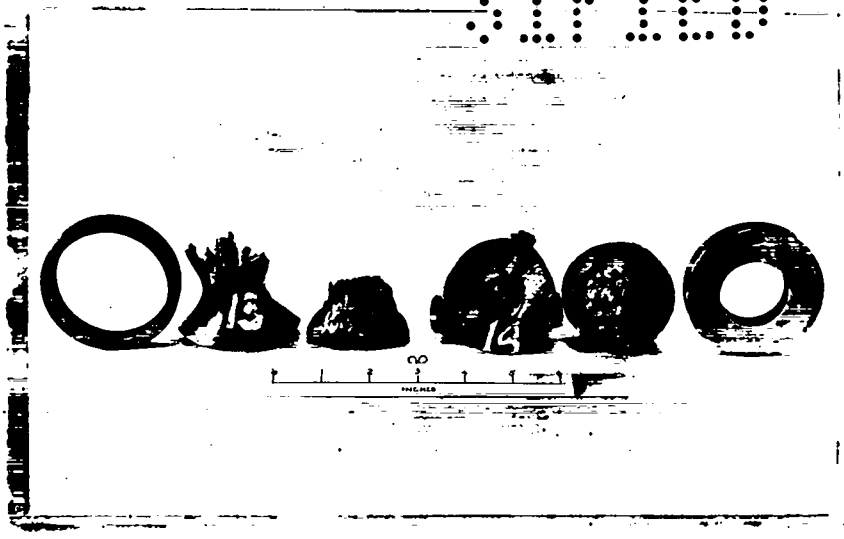

Fig. 16. Exp. 13: 3" OD, $\frac{1}{2}$" wall, 8" long
Comp. C, $1\frac{1}{2}$" thick, $7\frac{1}{2}$" long
Cf. Fig. 11, note uniform collapse when excessive charge is used

Exp. 14: 3" OD, $\frac{3}{4}$" wall, 8" long
Comp. C, $1\frac{1}{2}$" thick, $7\frac{1}{2}$" long
Plastic flow can be seen through end of cylinder

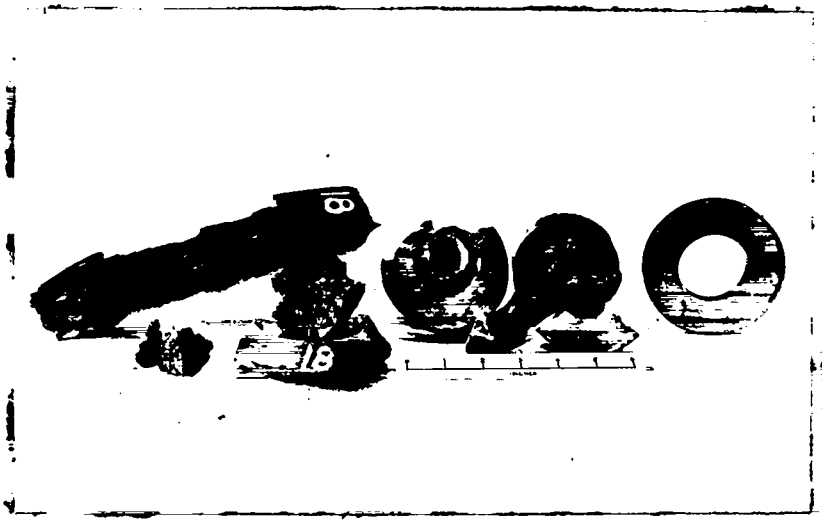

Fig. 17. Exp. 18: 4" OD, 1" wall, 12" long
Comp. C, 1" thick, $11\frac{1}{2}$" long. The pinching off of the ends with an approximately triangular section is typical. The long fragments show complete collapse before fragmentation. The somewhat porous appearance of the fragments is probably indicative of the release of a considerable ~~energy stored in elastic~~ compression.

Fig. 18. Exp. 26: 6" OD, 1" wall, 12 3/16" long
Comp. C, ¾" thick, 12 11/16" long

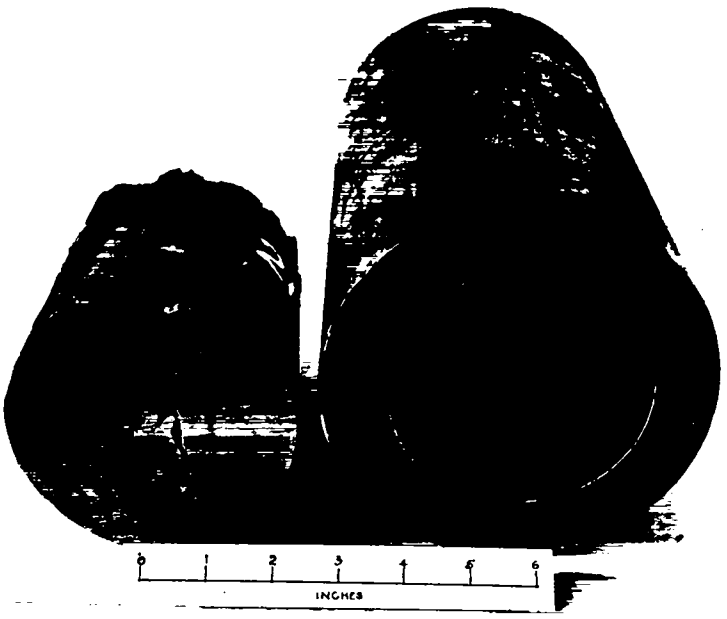

Fig. 19. Exp. 21: 6" OD, 1" wall 12" long
Comp. C, 1" thick, 11½" long